Two energy gaps in the tunneling-conductance spectra of the superconducting clathrate Ba_8Si_{46}

Yves Noat, Tristan Cren, Pierre Toulemonde, Alfonso San Miguel, François Debontridder, Vincent Dubost, and Dimitri Roditchev

Institut des Nanosciences de Paris, Université Pierre et Marie Curie-Paris 6, CNRS-UMR 7588, 4 place Jussieu, 75252 Paris, France; Institut Néel, CNRS et Université Joseph Fourier, 25 Avenue des Martyrs, BP 166, F-38042 Grenoble Cedex 9, France; and Laboratoire de Physique de la Matière Condensée et Nanostructures, CNRS UMR-5586, Université Claude Bernard Lyon 1, 43 Bld du 11 Novembre 1918, 69622 Villeurbanne, Lyon, France

(Received 29 September 2009; revised manuscript received 13 January 2010; published 19 March 2010)

We have studied the quasiparticle excitation spectrum of the superconductor Ba_8Si_{46} by local tunneling spectroscopy. Using high-energy resolution achieved in superconductor-insulator-superconductor junctions we observed tunneling conductance spectra of a nonconventional shape revealing two distinct energy gaps, $\Delta_L = 1.3 \pm 0.1$ meV and $\Delta_S = 0.9 \pm 0.2$ meV. The analysis of tunneling data identified Δ_L as the leading superconducting gap in the bulk material. A smaller and more dispersive gap Δ_S is interpreted as induced either in reciprocal space, via the quasiparticle interband scattering from the leading superconducting band, or in real space, by the proximity effect to a normal layer at the surface.

DOI: 10.1103/PhysRevB.81.104522 PACS number(s): 74.25.F−, 74.25.Dw, 74.50.+r

I. INTRODUCTION

In their microscopic theory of superconductivity[1] Bardeen, Cooper, and Schrieffer (BCS) predicted the existence of a single gap Δ in the elementary excitation spectrum of a superconductor (SC). However, already in late 1960s, some superconductors from the A15 family did show anomalies in specific heat that could be attributed to the presence of several energy gaps.[2,3] The existence of two energy gaps has also been suggested for Nb, Ta, and V.[4] Recent discovery of the two distinct SC gaps in MgB_2 reported in specific heat[5] and scanning tunneling microscopy/spectroscopy (STM/STS) experiments,[6–8] with the excitation spectrum deviating from the BCS, strongly renewed the interest for nonstandard superconductors.[9–12]

Among the covalent sp^3 materials, such as silicon carbide or silicon (or carbon) diamond, the silicon clathrate Ba_8Si_{46} appears to be a good candidate for a nonconventional superconductivity. This doped clathrate is formed by covalent Si_{20} and Si_{24} cages sharing their faces and filled with intercalated Ba atoms (for more details, see Ref. 13). It has been shown that the superconductivity appearing in Ba_8Si_{46} at $T_c = 8.1$ K (Refs. 14–18) is mediated by phonons and is an intrinsic property of the sp^3 network formed by Si atoms.[17] Eight encaged Ba atoms per unit cell provide the charge carriers[19] resulting in a complex band structure with several bands crossing the Fermi level. Thus, one could expect the superconductivity to be more or less developed in the different bands and to depend strongly on the interband scattering. Up to now however, the question remained a subject of controversy: Tanigaki *et al.*[18] concluded on a conventional BCS superconductivity in Ba_8Si_{46}, while tunneling spectroscopy data evidenced for an anisotropic order parameter,[20] and recent results of specific-heat measurements were reported to be consistent with two-gap superconductivity.[12]

In this paper we report the local tunneling spectroscopy (TS) of Ba_8Si_{46} performed in the STM geometry. In order to enhance the energy resolution, we studied superconductor-vacuum-superconductor (SIS) tunneling junctions formed by *in situ* cleaved Ba_8Si_{46} grains (used as STM tips) (Ref. 6) and a clean surface of 2H-$NbSe_2$. Such specific geometry allowed us to obtain high-quality tunneling junctions using available small granular Ba_8Si_{46} samples. Ba_8Si_{46}-vacuum-Ba_8Si_{46} SIS junctions were realized by gently crashing and then retracting the Ba_8Si_{46} tips into/from the surface of 2H-$NbSe_2$.

Statistical analysis of the SIS spectra revealed the existence of two energy gaps. A large one $\Delta_L = 1.3 \pm 0.1$ meV, giving a ratio $2\Delta_L/kT_c = 3.7 \pm 0.3$ comparable with the BCS value, is unambiguously attributed to the superconductivity in the bulk Ba_8Si_{46} material. A smaller one $\Delta_S = 0.9 \pm 0.2$ meV, appearing in the tunneling spectra of a nonconventional shape may, in principle, have two distinct origins. From one side, it could reflect the superconductivity induced in an intrinsically nonsuperconducting surface layer by proximity to the bulk Ba_8Si_{46}. From another side, the small gap may arise in an intrinsically nonsuperconducting electronic band of Ba_8Si_{46} by the interband quasiparticle scattering from another (leading) superconducting band. In the latter scenario Ba_8Si_{46} material is a two-gap superconductor.

II. TUNNELING-SPECTROSCOPY EXPERIMENTS

Polycrystalline Ba_8Si_{46} samples were synthesized at high pressure and temperature.[14,19] The Ba_8Si_{46} tips were fabricated by gluing a small grain of the material at the apex of a standard Pt/Ir tip. The grains were then fractured prior tunneling-spectroscopy experiment in order to expose a clean surface facing the STM junction (see insets in Figs. 1 and 2). In this work, both *ex situ* and *in situ* fractured Ba_8Si_{46} tips were studied. As a control of the tip quality, the ability of the tips to image Au or $NbSe_2$ surfaces was systematically checked. We also visualized the vortex lattice in $NbSe_2$ (Fig. 2) and observed the voltage-dependent contrast expected for high-quality SIS junctions.[21] This is an indication of both the *vacuum tunneling* regime and the *clean surfaces* of the tunneling electrodes. The raw $I(V)$ data acquired at tunneling

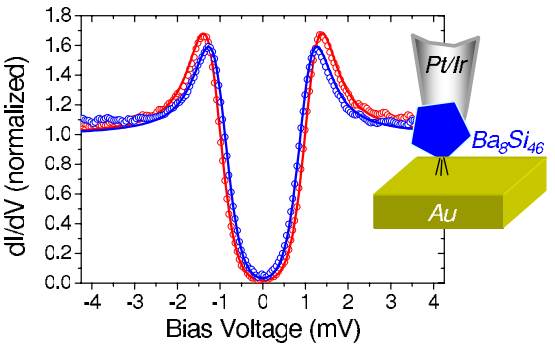

FIG. 1. (Color online) Two typical SIN tunneling conductance spectra obtained with a Ba_8Si_{46} tips and Au sample [red (gray) and blue (black) dots] at 2.3 K. Solid lines: best fits using Schopol & Scharnberg-McMillan equations [Eq. (5)] with $\Delta_1^0=0.08$ meV, $\Gamma_{12}=10$ meV, $\Delta_2^0=1.2$ meV, $\Gamma_{21}=1.49$ meV for the red (gray) curve and $\Delta_1^0=0.05$ meV, $\Gamma_{12}=11$ meV, $\Delta_2^0=1.33$ meV, $\Gamma_{21}=1.31$ meV for the blue (black) curve. Inset: schematic drawing of the experimental geometry.

resistances 10–100 MΩ were numerically derived and the resulting $dI(V)/dV$ spectra are presented normalized to unity for clarity.

Before focusing on the SIS spectroscopy, we first present in Fig. 1 typical superconductor insulator normal metal (SIN) tunneling conductance spectra obtained with Ba_8Si_{46}/Au

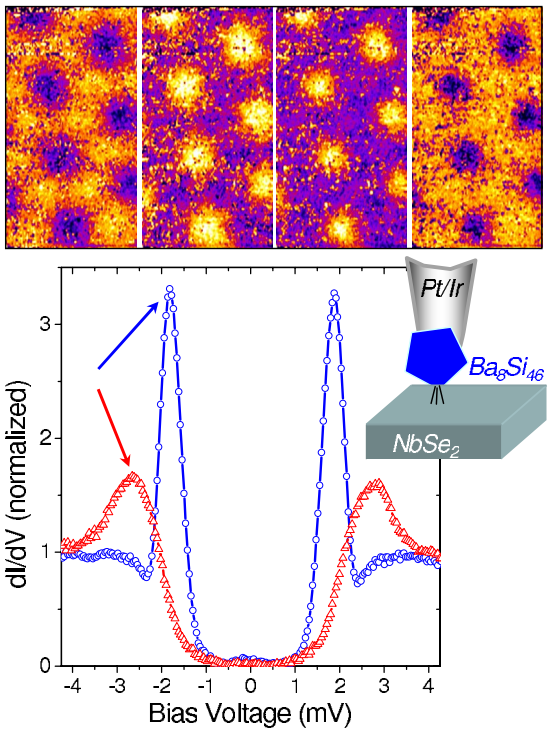

FIG. 2. (Color online) Ba_8Si_{46} vs $NbSe_2$ SIS spectra at $T=2.3$ K. The spectra reveal two distinct energy gaps in Ba_8Si_{46} (showed with arrows): $\Delta_S \simeq 0.8$ meV for the blue (black) curve and $\Delta_L \simeq 1.4$ meV for the red (gray) curve. Above: vortex lattice in $NbSe_2$ at $B=0.165$ T revealed with a Ba_8Si_{46} tip at several biases (from left to right) −2.0, −0.9, +1.0, and +1.9 mV showing the contrast inversion characteristic of SIS junctions (Ref. 21).

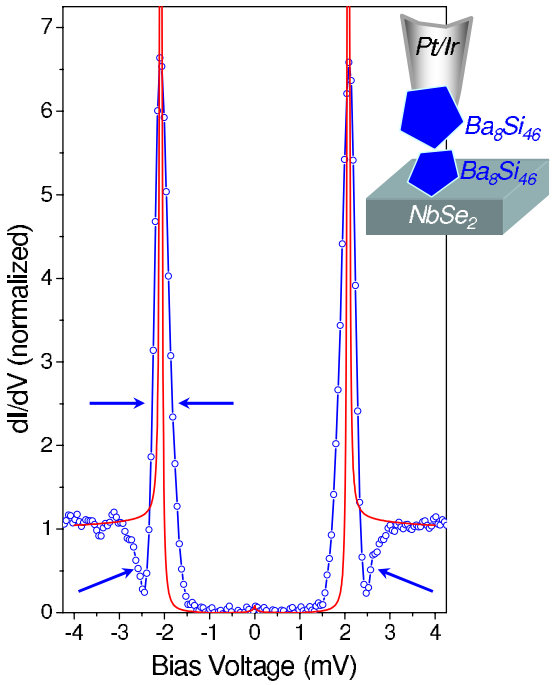

FIG. 3. (Color online) A typical Ba_8Si_{46} vs Ba_8Si_{46} SIS tunneling conductance spectrum [circled blue (black) curve]. A pure BCS fit, red (gray) line, clearly fails to reproduce the dips and the broadened quasiparticle peaks (pointed with arrows).

tunneling junctions. The spectra exhibit a smooth apparent gap $\Delta_{Ba_8Si_{46}} \simeq 1.0$ meV with no additional spectroscopic features visible. The position of the peaks varies (typically ± 0.2 mV) from one grain to another. Such thermally broadened SIN spectra are quite identical to those previously reported,[20] and which were interpreted as resulting from the anisotropy of the SC gap in the bulk. Nevertheless, the thermal broadening of $\simeq 3.5kT$ inherent to the SIN spectroscopy strongly impairs the energy resolution of TS at 2.3 K, giving one no chance to reveal fine spectroscopic features in the density of states (DOS). To overcome the thermal broadening limitation we applied SIS spectroscopy and thus considerably enhanced the energy resolution.

A typical Ba_8Si_{46}-$NbSe_2$ SIS spectrum is presented as the dotted blue (black) curve in Fig. 2. In SIS configuration the peaks appear at the position $\Delta_{peak}=\Delta_{NbSe_2}+\Delta_{Ba_8Si_{46}}$. Considering $\Delta_{NbSe_2}(T=2.2\ \text{K}) \simeq 1.1$ meV leads to $\Delta_{Ba_8Si_{46}} \simeq 0.8$ meV. The peaks are clearly better resolved than with SIN spectroscopy (Fig. 1). The SIS tunneling spectra are even sharper with Ba_8Si_{46}-Ba_8Si_{46} SIS junctions, as shown in Fig. 3 [circled blue (black) curve]. The peaks sharpness obtained both with $NbSe_2$ and Ba_8Si_{46} counterelectrodes clearly demonstrates the effect of enhanced energy resolution in SIS tunneling spectroscopy with respect to SIN geometry. The pure-BCS fit of the Ba_8Si_{46}-Ba_8Si_{46} spectrum [red (gray) solid line in Fig. 3] gives $\Delta_{Ba_8Si_{46}}=1.04$ meV. Thus, both SIN and SIS data in Figs. 1–3 reveal a gap value of $\Delta_{Ba_8Si_{46}}=0.9\pm0.2$ meV, corresponding to $2\Delta_{Ba_8Si_{46}}/kT_c = 2.6 < 3.52$ which is much too low to account for the superconductivity in bulk Ba_8Si_{46}. Furthermore, the standard BCS fit [red (gray) line in Fig. 3] fails to account for strongly

broadened quasiparticle peaks and local minima—*dips* (marked by arrows).[22] Both the low gap energy and the nonconventional shape of the tunneling spectra suggest the existence of another, larger SC gap Δ_L, responsible for the superconductivity in the bulk Ba_8Si_{46}, that is, hidden in the tunneling data for some reasons to determine. Hence, we have now to understand the origin(s) of the small gap Δ_S we do observe in TS and get some insight on a hypothetical hidden larger gap Δ_L.

In the following section we discuss two phenomena that indeed lead to the appearance of an additional (secondary) gap in superconductors. The first idea is to consider that two (or more) electronic bands are involved in superconductivity, each being characterized by a SC gap and thus, Ba_8Si_{46} is a multiple-gap superconductor. The second one is to suggest the existence of an intrinsically nonsuperconducting "dead" layer at the surface of Ba_8Si_{46} to which the superconductivity is induced by proximity effect to the bulk.

III. TWO-GAP SUPERCONDUCTIVITY VS PROXIMITY EFFECT

The necessity of a precise description of realistic SCs stimulated an important piece of theoretical effort. In 1959 Suhl, Matthias, and Walker (SMW) (Ref. 23) extended the one-band isotropic BCS model to the case of two energy bands. In their simple heuristic model each band has its own BCS Hamiltonian and a coupling term that scatters pairs from one band to another is added in order to couple both bands. This coupling is described by the partial Hamiltonian,

$$V_{12}\sum_{kk'} c^+_{k\uparrow}c^+_{-k\downarrow}d_{-k'\downarrow}d_{k'\uparrow} + d^+_{k\uparrow}d^+_{-k\downarrow}c_{-k'\downarrow}c_{k'\uparrow},$$

where c^+, c, d^+, d are the corresponding creation and annihilation operators in each band and V_{12} is the interband pair coupling. Such a model leads to a two-band SC that exhibits two distinct gaps in its excitation spectrum, Δ_1 and Δ_2 that are solutions of the self-consistent equations,

$$\Delta_1[1 - V_{11}N_1F(\Delta_1)] = \Delta_2 V_{12}N_2F(\Delta_2),$$

$$\Delta_2[1 - V_{22}N_2F(\Delta_2)] = \Delta_1 V_{12}N_1F(\Delta_1), \tag{1}$$

where

$$F(\Delta) = \int_0^{\hbar\omega_D} d\epsilon \tanh\left[\frac{\sqrt{\epsilon^2+\Delta^2}}{2k_BT}\right]/\sqrt{\epsilon^2+\Delta^2}. \tag{2}$$

$N_i = N_i(E_F)$, $i=1,2$, is the normal state DOS at the Fermi level in each band. The terms V_{11} and V_{22} are the usual BCS pair coupling in each band. The corresponding density of states is a weighted sum of two BCS spectra,

$$N_S(E) = \sum_{i=1,2} N_i(E_F)\mathrm{Re}\frac{|E|}{\sqrt{E^2-\Delta_i^2}}. \tag{3}$$

In tunneling experiments the tunneling probability is **k** dependent, hence the amount of tunneling electrons should be ponderated by an average tunneling probability to each band. Combining both the SMW model and tunneling selectivity, we shall expect an effective tunneling density of states should of the form,

$$N_S(E) = \sum_{i=1,2} W_i N_i(E_F)\mathrm{Re}\frac{|E|}{\sqrt{E^2-\Delta_i^2}}, \tag{4}$$

where W_i accounts for the k-averaged tunneling probability toward each band.

Let us point out that such a tunneling density of states [Eq. (4)] is nothing but a weighted sum of two BCS DOSs: It neither thinners the quasiparticle peaks nor generates the dips in SIS spectra. Thus SMW model fails to describe our experimental data. Nevertheless, the two-band model can be extended to give a more realistic description of multiple-band superconductivity. The first improvement consists in taking into account the interband quasiparticle scattering, nonaccounted for in SMW model. Schopol & Scharnberg (S&S) (Ref. 24) showed that the quasiparticle scattering in a two-band SMW superconductors leads to energy-dependent gap functions $\Delta_i(E)$ that depend essentially on the interband scattering times $\tau_{12} \sim 1/\Gamma_{12}$ and $\tau_{21} \sim 1/\Gamma_{21}$. The detailed balance equation requires that $N_1\Gamma_{12} = N_2\Gamma_{21}$. The gap functions are solutions of the coupled equations,

$$\Delta_1(E) = \frac{\Delta_1^0 + \Gamma_{12}\Delta_2(E)/\sqrt{\Delta_2^2(E) - (E - i\Gamma_{21})^2}}{1 + \Gamma_{12}/\sqrt{[\Delta_2^2(E) - (E - i\Gamma_{21})^2]}},$$

$$\Delta_2(E) = \frac{\Delta_2^0 + \Gamma_{21}\Delta_1(E)/\sqrt{\Delta_1^2(E) - (E - i\Gamma_{12})^2}}{1 + \Gamma_{21}/\sqrt{[\Delta_1^2(E) - (E - i\Gamma_{12})^2]}}, \tag{5}$$

where Δ_1^0 and Δ_2^0 are the gaps obtained from the self-consistency equations,

$$\Delta_i^0 = \lambda_{ii}\int_0^{\hbar\omega_i} dE \tanh\left[\frac{E}{2k_BT}\right]\mathrm{Re}\left[\frac{\Delta_i(E)}{\sqrt{E^2-\Delta_i^2(E)}}\right] + \lambda_{ij}\sqrt{\frac{N_j}{N_i}}\int_0^{\hbar\omega_{ij}} dE \tanh\left[\frac{E}{2k_BT}\right]\mathrm{Re}\left[\frac{\Delta_i(E)}{\sqrt{E^2-\Delta_i^2(E)}}\right], \tag{6}$$

where $\lambda_{ii} = V_{ii}N_i$ are the intraband electron-phonon coupling constants, while $\lambda_{ij} = V_{ij}\sqrt{N_iN_j}$ is the interband electron-phonon coupling constant of the SMW model.

The partial density of state with the energy-dependent gap functions are given by

$$N_{\mathrm{Si}}(E) = N_i(E_F)\mathrm{Re}\frac{|E|}{\sqrt{E^2-\Delta_i^2(E)}}. \tag{7}$$

As shown in Ref. 24 the quasiparticle scattering leads to rounded quasiparticle peaks. In addition, bumps appear in the two partial densities of states. Such structures were indeed observed in MgB_2 and perfectly described in the framework of S&S model by Schmidt *et al.*[8]

Experimentally, the tunneling experiments probe the electronic properties at the very surface of studied samples, which may, in principle, differ from their bulk counterpart. Indeed, the surface is a defect that may affect the local density of states. First, the translational invariance perpendicular to the surface is broken, which may lead to the formation of

particular surface states, such as Shockley or Tamm states,[25,26] that do not exist in the bulk. This may also give rise to some reconstruction and appearance of dangling bonds that may induce a particular electronic structure, different from the bulk, in a thin surface layer. The surface is also the place where oxidation and hydroxylation take place in the first stage. Hence, in many cases the surface electronic properties are not identical to the bulk ones and surface sensitive techniques might be flawed. In the case where a multigap superconductivity is presumed, this is a very stringent problem, since the equations of the energy-dependent gap functions [Eq. (5)] of a two-gap superconductor are *formally identical* to the ones derived for the proximity effect by McMillan.[27]

In his treatment of superconducting proximity effect between two metallic films, McMillan started from two initial BCS gaps in each band Δ_1^0 and Δ_2^0 and added a Bardeen-type tunneling coupling between both metals, leading to coupling energies Γ_{12} and Γ_{21} accounting for the quasiparticle scattering from one metal to the other. Here the detailed balance impose $N_1 d_1 \Gamma_{12} = N_2 d_2 \Gamma_{21}$, where d_1 and d_2 are the thickness of the two films that are supposed thin with respect to the coherence length ξ: $d_1, d_2 \ll \xi$. With these assumptions one recovers the Eq. (5) of the energy-dependent gaps $\Delta_1(E)$ and $\Delta_2(E)$ of the S&S two-gap model.

This analogy between proximity effect and two-gap superconductivity is due to the fact that quasiparticle scattering in real space or reciprocal space are described by the same way when the film thickness, where proximity effect takes place, is much thinner than the characteristic scale ξ. The similarity between multigap superconductivity and proximity effect is even more profound since the McMillan proximity model, that considers quasiparticle scattering, and the SMW two-gap model, that suppose Cooper-pair scattering, have strong similarities. Indeed, Noce and Maritato[28] demonstrated that assuming a simplified solution of the McMillan proximity model with nonenergy-dependent gap function $\Delta_i(E) = \Delta_i$ they recovered the same self-consistent gap equations than in the SMW model [Eq. (1)]. Note however that SMW and McMillan models differ in one important point: in SMW a pure interband pair coupling V_{12} leads to superconductivity even with zero intraband coupling $V_{11} = V_{22} = 0$, while in the McMillan proximity model, a quasiparticle coupling between two nonsuperconducting metals would not induce superconductivity.

The formal identity between the S&S reciprocal-space two-gap superconductivity and McMillan's real-space proximity effect strongly complicates the interpretation of TS data. However, one can exploit the fact that the ratio Γ_{12}/Γ_{21}, constant and equal to N_2/N_1 in S&S approach, is thickness dependent in the McMillan proximity model: $\Gamma_{12}/\Gamma_{21} = \frac{N_2 d_2}{N_1 d_1}$. Hence, in the proximity case, the Γ_{12}/Γ_{21} ratio should vary from sample to sample and from one location to another depending on the particular thickness of the proximity layer.

In Figs. 4(a) and 4(b) we show the partial DOSs $N_{Si}(E)$ calculated in the framework of S&S two-gap model for an intrinsically nonsuperconducting band $i=1$: $\Delta_1^0 = 0$ meV, coupled to an intrinsically superconducting band $i=2$: $\Delta_2^0 = 1.3$ meV. Different curves corresponding to the coupling

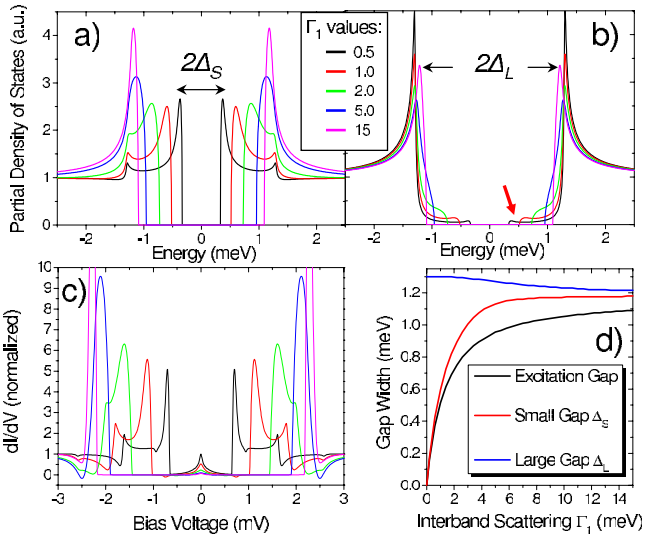

FIG. 4. (Color online) Partial DOSs in the band 1 in (a) and 2 in (b) calculated within the McMillan model with $\Delta_1^0 = 0$, $\Delta_2^0 = 1.3$ meV, $\Gamma_1 = 0.5$, 1, 2, 5, and 15 meV and $\Gamma_2 = \Gamma_1/10$. (c) Evolution of the excitation gap and apparent gaps Δ_L, Δ_S with the scattering rate Γ_1, corresponding to (a) and (b). In (c), simulated conductance spectra at 2.3 K are shown for a SIS junction with both electrodes exhibiting the DOS of the small gap band shown in (a). The plot (d) shows the evolution of the excitation gap and the peak-to-peak gaps Δ_S and Δ_L in the small gap and large gap band, as a function of the coupling Γ_1.

parameters Γ_{12} varying from 0.5 to 15 meV with a constant ratio $\Gamma_{12}/\Gamma_{21} = 10$, that corresponds to the typical range of parameters found for Ba_8Si_{46} (see below). These calculated densities of states could also represent the proximity case between a metallic film ($i=1$) in close contact with a superconducting film $i=2$, in the framework of McMillan model. As a result of the interband (or intermetal) quasiparticle scattering, a gap Δ_S is induced in the first band (or proximity layer) where it does not exist at zero coupling. The DOS shape in the first band (or proximity layer) is very peculiar [Fig. 4(a)]: the quasiparticle peaks are broadened and there are some shoulders at the position of the large gap peaks. This peculiar shape is responsible for the appearance of dips in SIS spectra. This is illustrated in Fig. 4(c) where simulated SIS tunneling spectra supposing that both electrodes exhibit the small induced gap of Fig. 4(a). The key point is that there is a clear signature of the presence of a (hidden) larger gap whatever the phenomenon considered. It features as a dip in SIS spectra for strong enough couplings. The curve corresponding to $\Gamma_1 = 5$ meV shows that the dips may even become negative in the SIS spectra while no dips are present in the initial DOS.

In the large gap band (or superconducting film) the initially pure BCS DOS evolves with the coupling [Fig. 4(b)]: a minigap (often called "excitation gap") appears at the same position that the induced gap in the first band as shown by the red arrow in Fig. 4(b). Thus, different apparent gaps appear in the model. The excitation gap, that corresponds to the excitations of lowest energies, is close to the peak-to-peak value of the small induced gap that will be defined as $2\Delta_S$. The second important gap is defined as peak-to-peak value

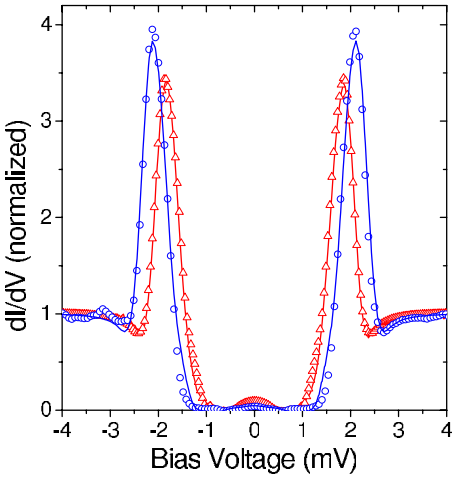

FIG. 5. (Color online) Typical Ba_8Si_{46} vs $NbSe_2$ SIS tunneling conductance spectra [red (gray) triangles and blue (black) circles] observed at $T=2.2$ K. Solid lines: best SIS fits with Schopol & Scharnberg-McMillan equations [Eq. (5)] with the following parameters: for the red (gray) curve: $\Delta_1^0=0.0$ meV, $\Gamma_{12}=2.2$ meV, $\Delta_2^0=1.1$ meV, and $\Gamma_{21}=0.17$ meV, and for the blue (black) curve $\Delta_1^0=0.07$ meV, $\Gamma_{12}=3.54$ meV, $\Delta_2^0=1.34$ meV, and $\Gamma_{21}=0.26$ meV. The DOS of $NbSe_2$ used for the fits was taken from Ref. 29.

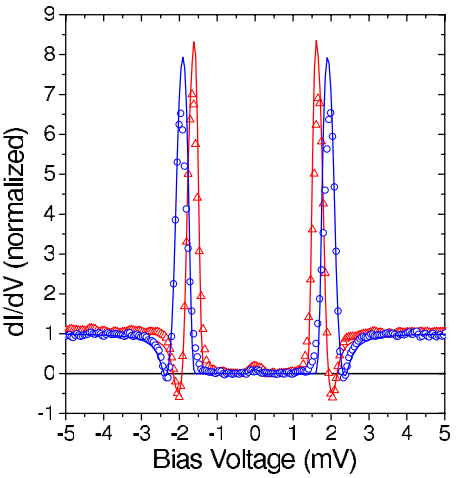

FIG. 6. (Color online) Typical Ba_8Si_{46} vs Ba_8Si_{46} SIS tunneling conductance spectra [red (gray) triangles and blue (black) circles] observed at $T=2.2$ K. In some junctions a negative tunneling conductance is measured at the dip positions (arrows). Solid lines: best SIS fits with Schopol & Scharnberg-McMillan model obtained with the following parameters: for the red (gray) curve $\Delta_1^0=0.0$ meV, $\Gamma_{12}=2.6$ meV, $\Delta_2^0=1.1$ meV, and $\Gamma_{21}=0.18$ meV; and for the blue (black) curve $\Delta_1^0=0.0$ meV, $\Gamma_{12}=3.7$ meV, $\Delta_2^0=1.23$ meV, and $\Gamma_{21}=0.40$ meV.

$2\Delta_L$ in the large gap band. The evolution of the excitation gap, of the induced small gap Δ_S and of the leading gap Δ_L as a function of the coupling parameter Γ_{12} is presented in Fig. 4(d). Both gaps Δ_S and Δ_L vary strongly at moderate Γ_{12} and reach the same asymptotic value for very large coupling, where one recovers a simple one-gap BCS DOS as expected from the Anderson's theorem.

IV. FITS TO THE DATA

In Figs. 5 and 6 we present fitted SIS tunneling spectra of Ba_8Si_{46}-$NbSe_2$ and Ba_8Si_{46}-Ba_8Si_{46} junctions, respectively. The Fig. 7(a) shows the temperature dependence of the later. The enhanced energy resolution of SIS spectroscopy revealed the apparent gap $\Delta_{Ba_8Si_{46}}$ to vanish exactly at the T_c of the bulk material [Fig. 7(b)], thus evidencing an intimate connection of the observed gap to the bulk SC. The SIS fits using Schopol & Scharnberg-McMillan equations [Eq. (5)], shown as solid lines in Figs. 5–7, reproduce in fine details the shape of the SIS tunneling conductance data, with different counterelectrode materials and at various temperatures [red (gray) lines in Fig. 7]. A perfect agreement is also achieved when fitting SIN spectra (solid lines in Fig. 1). In the case of $NbSe_2$ as a counterelectrode (Fig. 5), the fits were done assuming the tunneling DOS taken from Rodrigo & Viera[29] who proceeded to a very fine measurement of the tunneling DOS of $NbSe_2$ by SIS spectroscopy with a Pb tip.

By analyzing the fitting parameters of different tunneling spectra we noticed the following common features: (1) for all spectra, the initial BCS gap in the band $i=1$ is $\Delta_1^0 \approx 0$ meV while $\Delta_2^0=1.3\pm0.1$ meV. (2) The interband scattering parameters, Γ_{12} and Γ_{21}, strongly vary from one junction to another, but their ratio remains almost fixed $\Gamma_{12}/\Gamma_{21} \sim 10$ as shown in Fig. 8. (3) For most of the studied junctions, the tunneling contribution of the band $i=1$ was $W_1=1$ and that of $i=2$ was $W_2=0$, i.e., we needed only the partial density of state of the small gap $N_{S1}(E)$ to fit the tunneling spectra.

Thus, assuming $\Gamma_{21}=\Gamma_{12}/10$ only two variable parameters remained, Δ_2^0 and Γ_{12}. Moreover, the fits of the temperature-dependent spectra in Fig. 7(a) were generated considering only one free parameter, $\Delta_2^0(T)$, the second $\Gamma_{12}=6$ meV being evaluated once for all at $T=2.2$ K and kept fixed up to the critical temperature.

Let us now discuss the physics behind such a surprisingly nice agreement between the data and fits, and analyze the consequences of the above-mentioned common features. The condition $\Delta_1^0 \approx 0$ meV implies that the superconductivity in the band $i=1$ (or in the surface layer, within McMillan hypothesis) is fully induced: A small gap opens in $N_{S1}(E)$ due to the coupling with the leading superconducting band $i=2$ where the pairing amplitude $\Delta_2^0 \simeq 1.3\pm0.1$ meV is found close to the value 1.4 meV estimated from specific-heat measurements.[12] The observed fluctuations of the induced small gap Δ_S from one junction to another, on the order of ±0.2 meV, are attributed to the variations in both the scattering rates Γ_i and the pairing amplitude of the initial leading gap Δ_2^0.

While at this point we cannot discriminate between two possible origins of our observations (a two-gap scenario or a simple proximity effect in a metallic surface layer), we note that two-gap superconductivity has already been inferred in Ba_8Si_{46} by Lortz *et al.*[12] on the basis of specific-heat measurements. Nevertheless, there is a large discrepancy between the small gap measured by tunneling spectroscopy $\Delta_S=1$ meV and the one determined by specific-heat measurements $\Delta_S=0.35$ meV. However, a larger scattering due

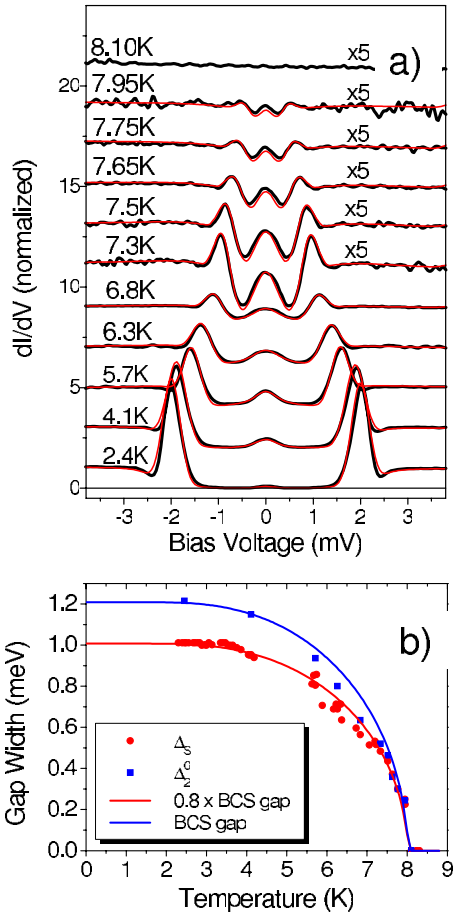

FIG. 7. (Color online) (a) Temperature dependence of the Ba_8Si_{46} vs Ba_8Si_{46} SIS spectra in black and their fits in red (gray) using Schopol & Scharnberg-McMillan model. The spectra are shifted for clarity. In (b) temperature dependence of the peak-to-peak gap extracted from Ba_8Si_{46} vs Ba_8Si_{46} SIS spectra.

to a enhanced disorder near the crystal surface may easily explain the differences between these two measurements of the small gap in Ba_8Si_46. Indeed, the value $\Delta_S=0.35$ meV can be obtained within S&S model considering the $\Delta_2^0 \simeq 1.3$ meV we found together with a smaller

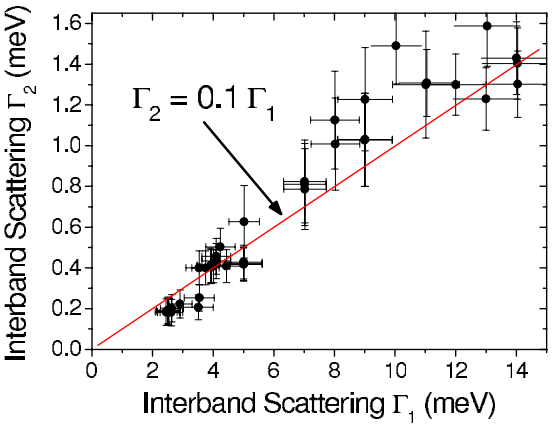

FIG. 8. (Color online) Scatter plot of the fit parameters Γ_2 vs Γ_1. Red (gray) line: linear dependence $\Gamma_2=\Gamma_1/10$.

$\Gamma_{12}=0.6$ meV for the bulk and the ratio $\Gamma_1/\Gamma_2 = N_2(E_F)/N_1(E_F)=10$ estimated from the ratio of the density of states determined by specific-heat measurements.

We note that broad peaks and dips were also observed in high-T_c SCs and attributed to the coupling with a collective excitation mode.[30–32] Nevertheless, the dips predicted by S&S model are not equivalent to those observed in cuprates. First of all, Ba_8Si_{46} is not a strongly correlated material and strong electron-electron correlations are not expected there. Second, in the cuprate case the dips are directly present in the SIN TS spectra, while in S&S model they are so weak in the DOS, that they only appear in SIS spectra due to a convolution effect in the tunneling integral.

V. ANALYSIS WITHIN S&S TWO-BAND MODEL

The fit to the data with S&S model using Eq. (5) leads to the following gap parameters $\Delta_1^0 \simeq 0$ and $\Delta_2^0 \simeq 1.3$. With such gap values the self-consistency equations in the framework of S&S model [Eq. (6)] lead necessarily to $\lambda_{11}=V_{11}N_1=0$ and $\lambda_{12}=V_{12}\sqrt{N_1N_2}=0$. Assuming that the Ba phonon rattling modes are the principal contributors to the SC pairing[12,33] we take a cutoff frequency of $\hbar\omega \simeq 7$ meV that leads to $\lambda_{22}=V_{22}N_2=0.42$. This value corresponds to a rather strong-coupling regime but is however quite smaller than $\lambda_{e\text{-}ph} \simeq 0.7$ obtained by Lortz *et al.*[12] This is not surprising since we assumed a rather simplified pairing potential.

In the framework of the simple SMW model, $\Delta_1^0 \simeq 0$ would mean that the small gap is completely closed. However this is not the case experimentally. Indeed, a small gap opens in band 1, and assuming a two-gap scenario, this can only be due to the interband quasiparticle scattering described by the S&S model. In order to describe the interband scattering, we assumed two free parameters Γ_{12} and Γ_{21}. In agreement with what we expected for a two-gap superconductor we found a clear linear correlation between Γ_{12} and Γ_{21} as evidenced in Fig. 8 with $\Gamma_{12}/\Gamma_{21} \sim 10$. This result gives a very strong argument for S&S two-gap scenario: The interband scattering events $1 \rightarrow 2$ and $2 \rightarrow 1$ should be equal and therefore, the condition $\Gamma_{12}/\Gamma_{21}=N_2(E_F)/N_1(E_F)$ must be fulfilled.[24] Moreover, we find the ratio ~ 10, in a very good agreement with the value $N_2(E_F)/N_1(E_F)=9$ determined from specific-heat measurements,[12] that strongly supports our model. In the framework of the band scenario, the variations in Γ_{12} and Γ_{21} may result of the specific scattering due to the local surface disorder, realized for each tunnel junction.

It is not fully established for the moment why the spectra revealing directly the large gap are so rare. In the case of MgB_2 a similar statistics was observed[34] and attributed to the low probability of tunneling into the two-dimensional π band. It is not clear if such an assumption holds for Ba_8Si_{46}. We know however that in Ba_8Si_{46} most of the DOS belongs to Ba-Si hybridized states located inside the Si cages.[18,19] It couples well to Ba phonon rattling modes that contribute to the SC pairing.[12,33] Hence, we may speculate that the electronic states responsible for the superconductivity are somehow confined inside the clathrate cages, and the amplitude of the corresponding evanescent waves outside the material is

thus weak, leading to a tiny contribution into the tunneling. Consequently, most of the tunneling current would come from the outer-cage Si orbitals where the superconductivity is purely induced.

In the search for a direct evidence of the large gap Δ_L, we studied several tens of Ba_8Si_{46} samples. We expected that the surface defects such as large steps, protrusions, holes would provide various tunneling conditions. In some measurements we indeed observed very different still reproducible SIS spectra [red (gray) curve in Fig. 1(c)] while keeping the tunneling conditions unchanged. They show no dips, as expected for SIS spectra revealing the large gap, Fig. 3(b). Furthermore, the gap energy $\Delta_L \approx 1.4$ meV corresponding to these spectra is in a good agreement with the large gap deduced from specific-heat measurements by Lortz *et al.*[12]

VI. ANALYSIS WITHIN THE PROXIMITY MODEL

As previously discussed, the McMillan equations describing the proximity effect are formally equivalent to S&S two-band model with interband quasiparticle scattering. Hence, the nice agreement between the TS data and the fits using Eq. (5) may also be interpreted in the framework of the proximity scenario, since the STS data may be affected by a surface layer, even in the situation where the sample were broken in UHV. Indeed, the crystal surface itself is a topological defect with respect to the bulk material, due to the crystal symmetry breaking. In some cases, it could even result in a new electronic band, present only at the surface [as it is the case of Cu(111) or Ag(111), for instance]. The superconductivity could be induced to this band by the coupling with the bulk SC, and thus the reduced gap Δ_S could, in principle, represent the surface state SC gap which would not extend to the bulk. Such hypothesis is generally valid for the surface of any SC and cannot be ruled out even for *in situ* prepared junctions.

In the McMillan model the ratio Γ_{12}/Γ_{21} is thickness dependent: $\Gamma_{12}/\Gamma_{21}=\frac{N_2 d_2}{N_1 d_1}$. Hence, this ratio should vary from sample to sample depending on the particular thickness of the proximity layer which is not the case as shown in Fig. 8. A constant ratio could only be explained assuming a constant thickness proximity layer inherent to the material. Nevertheless, with such an inherent, intrinsic, surface layer it seems difficult to understand the variations of 1 order of magnitude of the absolute value of Γ_{ij}. In the McMillan scenario the absolute value of the coupling depends on the transparency of the normal/superconductor interface. Then if the normal surface layer is intrinsic to the material, one could wonder where the variations on the interface transparency come from.

Before concluding, we note that the McMillan model is not perfectly appropriate for our purpose since it was devoted to the case of two thin film ($d \ll \xi$) in close contact while in our case the hypothetic non-SC metallic surface layer would be connected to a bulk superconductor. This problem of the local density of states in a dirty normal metal connected to a superconductor has been studied by Belzig *et al.*[35] using Usadel formalism. The more general case of the calculation of the DOS at the surface of a mesoscopic proximity layer from the clean to the dirty limit in the proximity layer has also been addressed by Pilgram *et al.*[36] using the Eilenberger formalism but these works are well beyond the scope of the present paper. Nevertheless, in our case the MacMillan equations may in fact be used considering an effective finite thickness of the superconductor on the order of ξ or a diffusion length $\sqrt{\xi l}$ depending on the mean-free path l in the bulk Ba_8Si_{46}.

VII. CONCLUSIONS

Finally, we have studied the quasiparticle excitation spectrum of the superconductor Ba_8Si_{46} by local tunneling spectroscopy. Owing high-energy resolution achieved in SIS junctions we resolved fine spectroscopic features that cannot be accounted for by BCS. The SIS spectra evidence the existence of two distinct energy gaps, $\Delta_L=1.3\pm0.1$ meV and $\Delta_S=0.9\pm0.2$ meV, that are interpreted in terms of a two-band superconductivity. The main conclusion is that the tunneling spectra in Ba_8Si_{46} are characterized by a leading gap of the bulk material, Δ_L: $2\Delta_L/kT_c=3.7\pm0.3$ and by another, smaller coupling-dependent gap Δ_S, reflecting a superconductivity induced in an intrinsically nonsuperconducting electronic band. Because of the extreme sensitivity of the tunneling spectroscopy to the electronic properties at the very surface, the proximity origin of the small gap Δ_S is not completely excluded. It does not alter, however, the result concerning the energy value and the bulk superconducting origin of the large gap Δ_L.

The methodology depicted in the paper may certainly be applied to other multigap superconductors. We showed that the excitation spectra of two-gap superconductors are particularly sensitive to disorder, in contrast with one-band BCS superconductors. Specifically, the amplitude of the smaller (induced) gap and the shape of the spectra strongly depend on the sample quality. Moreover, bulk sensitive methods and surface sensitive ones may give rather different values for the small gap since the quasiparticle scattering at the surface is usually stronger than that in the bulk.

[1] J. Bardeen, L. N. Cooper, and J. R. Schrieffer, Phys. Rev. **108**, 1175 (1957).

[2] J. C. F. Brock, Solid State Commun. **7**, 1789 (1969).

[3] V. Guritanu, W. Goldacker, F. Bouquet, Y. Wang, R. Lortz, G. Goll, and A. Junod, Phys. Rev. B **70**, 184526 (2004), and references therein.

[4] L. Yun Lung Shen, N. M. Senozan, and N. E. Phillips, Phys. Rev. Lett. **14**, 1025 (1965).

[5] F. Bouquet, Y. Wang, R. A. Fisher, D. G. Hinks, J. D. Jorgensen, A. Junod, and N. E. Phillips, Europhys. Lett. **56**, 856 (2001).

[6] F. Giubileo, D. Roditchev, W. Sacks, R. Lamy, D. X. Thanh, J. Klein, S. Miraglia, D. Fruchart, J. Marcus, and P. Monod,

Phys. Rev. Lett. **87**, 177008 (2001).
[7] G. Rubio-Bollinger, H. Suderow, and S. Vieira, Phys. Rev. Lett. **86**, 5582 (2001); P. Szabó, P. Samuely, J. Kacmarcík, T. Klein, J. Marcus, D. Fruchart, S. Miraglia, C. Marcenat, and A. G. M. Jansen, *ibid.* **87**, 137005 (2001).
[8] H. Schmidt, J. F. Zasadzinski, K. E. Gray, and D. G. Hinks, Physica C **385**, 221 (2003).
[9] B. Bergk, V. Petzold, H. Rosner, S.-L. Drechsler, M. Bartkowiak, O. Ignatchik, A. D. Bianchi, I. Sheikin, P. C. Canfield, and J. Wosnitza, Phys. Rev. Lett. **100**, 257004 (2008), and references therein.
[10] C. Dubois, A. Petrovic, G. Santi, C. Berthod, A. A. Manuel, M. Decroux, Ø. Fischer, M. Potel, and R. Chevrel, Phys. Rev. B **75**, 104501 (2007).
[11] I. Guillamón, H. Suderow, S. Vieira, L. Cario, P. Diener, and P. Rodière, Phys. Rev. Lett. **101**, 166407 (2008).
[12] R. Lortz, R. Viennois, A. Petrovic, Y. Wang, P. Toulemonde, C. Meingast, M. M. Koza, H. Mutka, A. Bossak, and A. San Miguel, Phys. Rev. B **77**, 224507 (2008).
[13] A. San Miguel and P. Toulemonde, High Press. Res. **25**, 159 (2005).
[14] P. Toulemonde, Ch. Adessi, X. Blase, A. San Miguel, and J. L. Tholence, Phys. Rev. B **71**, 094504 (2005).
[15] H. Kawaji, H. O. Horie, S. Yamanaka, and M. Ishikawa, Phys. Rev. Lett. **74**, 1427 (1995).
[16] S. Yamanaka, E. Enishi, H. Fukuoka, and M. Yasukawa, Inorg. Chem. **39**, 56 (2000).
[17] D. Connétable, V. Timoshevskii, B. Masenelli, J. Beille, J. Marcus, B. Barbara, A. M. Saitta, G.-M. Rignanese, P. Mélinon, S. Yamanaka, and X. Blase, Phys. Rev. Lett. **91**, 247001 (2003).
[18] K. Tanigaki, T. Shimizu, K. M. Itoh, J. Teraoka, Y. Moritomo, and S. Yamanaka, Nature Mater. **2**, 653 (2003).
[19] P. Toulemonde, A. San Miguel, A. Merlen, R. Viennois, S. Le Floch, C. Adessi, X. Blase, and J. L. Tholence, J. Phys. Chem. Solids **67**, 1117 (2006).
[20] K. Ichimura, K. Nomura, H. Fukuoka, and S. Yamanaka, Physica C **388-389**, 577 (2003).
[21] A. Kohen, Th. Proslier, T. Cren, Y. Noat, W. Sacks, H. Berger, and D. Roditchev, Phys. Rev. Lett. **97**, 027001 (2006).
[22] Note that Ba_8Si_{46}-Ba_8Si_{46} junctions do not contain any host material (as it is the case of Ba_8Si_{46}-$NbSe_2$ junctions). Thus, the observed deviations from BCS behavior are intrinsic to Ba_8Si_{46}.
[23] H. Suhl, B. T. Matthias, and L. R. Walker, Phys. Rev. Lett. **3**, 552 (1959).
[24] N. Schopohl and K. Scharnberg, Solid State Commun. **22**, 371 (1977).
[25] W. Shockley, Phys. Rev. **56**, 317 (1939).
[26] I. Tamm, Phys. Z. Sowjetunion **1**, 733 (1932).
[27] W. L. McMillan, Phys. Rev. **175**, 537 (1968).
[28] C. Noce and L. Maritato, Phys. Rev. B **40**, 734 (1989).
[29] J. G. Rodrigo and S. Vieira, Physica C **404**, 306 (2004).
[30] J. F. Zasadzinski, L. Ozyuzer, N. Miyakawa, K. E. Gray, D. G. Hinks, and C. Kendziora, Phys. Rev. Lett. **87**, 067005 (2001); L. Ozyuzer, J. F. Zasadzinski, N. Miyakawa, C. Kendziora, J. Sha, D. G. Hinks, and K. E. Gray, Physica C **341-348**, 927 (2000);
P. Romano, L. Ozyuzer, Z. Yusof, C. Kurter, and J. F. Zasadzinski, Phys. Rev. B **73**, 092514 (2006).
[31] T. Cren, D. Roditchev, W. Sacks, and J. Klein, Europhys. Lett. **52**, 203 (2000).
[32] N. Jenkins, Y. Fasano, C. Berthod, I. Maggio-Aprile, A. Piriou, E. Giannini, B. W. Hoogenboom, C. Hess, T. Cren, and Ø. Fischer, Phys. Rev. Lett. **103**, 227001 (2009).
[33] J. S. Tse, T. Iitaka, T. Kume, H. Shimizu, K. Parlinski, H. Fukuoka, and S. Yamanaka, Phys. Rev. B **72**, 155441 (2005).
[34] F. Giubileo, D. Roditchev, W. Sacks, R. Lamy, and J. Klein, Europhys. Lett. **58**, 764 (2002).
[35] W. Belzig, C. Bruder, and G. Schön, Phys. Rev. B **54**, 9443 (1996).
[36] S. Pilgram, W. Belzig, and C. Bruder, Phys. Rev. B **62**, 12462 (2000).